Powder Technology 214 (2011) 388–399

Contents lists available at SciVerse ScienceDirect

Powder Technology

journal homepage: www.elsevier.com/locate/powtec

Experimental study of cake formation on heat treated and membrane coated needle felts in a pilot scale pulse jet bag filter using optical in-situ cake height measurement

Mahmood Saleem [a,b,*], Rafi Ullah Khan [a], M. Suleman Tahir [b], Gernot Krammer [b]

[a] Institut of Chemical Engineering and Technology, University of the Punjab, Quaid-i-Azam Campus, 54590-Lahore, Pakistan
[b] Graz University of Technology, Graz, Austria

ARTICLE INFO

Article history:
Received 9 December 2010
Received in revised form 16 August 2011
Accepted 28 August 2011
Available online 3 September 2011

Keywords:
Cake formation
Needle felts
Bag filter
In-situ
Cake height measurements

ABSTRACT

Pulse-jet bag filters are frequently employed for particle removal from off gases. Separated solids form a layer on the permeable filter media called filter cake. The cake is responsible for increasing pressure drop. Therefore, the cake has to be detached at a predefined upper pressure drop limit or at predefined time intervals. Thus the process is intrinsically semi-continuous. The cake formation and cake detachment are interdependent and may influence the performance of the filter. Therefore, understanding formation and detachment of filter cake is important. In this regard, the filter media is the key component in the system. Needle felts are the most commonly used media in bag filters. Cake formation studies with heat treated and membrane coated needle felts in pilot scale pulse jet bag filter were carried out. The data is processed according to the procedures that were published already [Powder Technology, Volume 173, Issue 2, 19 April 2007, Pages 93–106]. Pressure drop evolution, cake height distribution evolution, cake patches area distribution and their characterization using fractal analysis on different needle felts are presented here. It is observed that concavity of pressure drop curve for membrane coated needle felt is principally caused by presence of inhomogeneous cake area load whereas it is inherent for heat treated media. Presence of residual cake enhances the concavity of pressure drop at the start of filtration cycle. Patchy cleaning is observed only when jet pulse pressure is too low and unable to provide the necessary force to detach the cake. The border line is very sharp. Based on experiments with limestone dust and three types of needle felts, for the jet pulse pressure above 4 bar and filtration velocity below 50 mm/s, cake is detached completely except a thin residual layer (100–200 μm). Uniformity and smoothness of residual cake depends on the surface characteristics of the filter media. Cake height distribution of residual cake and newly formed cake during filtration prevails. The patch size analysis and fractal analysis reveal that residual cake grow in size (latterly) following regeneration initially on the base with edges smearing out, however, the cake heights are not leveled off. Fractal dimension of cake patches boundary falls in the range of 1–1.4 and depends on vertical position as well as time of filtration. Cake height measurements with Polyimide (PI) needle felts were hampered on account of its photosensitive nature.

1. Introduction

Pulse jet bag filters are frequently employed for particle removal from off gases. The gas pervades through the permeable media while separated solids form a layer on the surface called the filter cake. The increasing cake thickness results in increasing pressure drop across the filter. The process is intrinsically semi-continuous since the filter media has to be re-generated either at predefined upper pressure drop limit or predefine time interval. The pressure drop depends on combined flow resistance of filter media and the cake, which varies with many factors like cake porosity, specific resistance, distribution of cake area load (cake mass per unit area), distribution of filtration velocity and filter media. Generally the average values of cake area load and filtration velocity are used whereas, in reality, both might be highly non uniform resulting in non uniform local flow distribution along the filter surface. As a result, the forming cake will possess different properties locally which may affect cake detachment. Patchy cleaning has been reported on both flexible and rigid filter media [1,2]. Since the performance of the bag house is strongly linked to the cake formation and regeneration, information on cake height distribution, size of cake patches and growth of cake patches is very important for understanding the cake formation phenomena, modeling the pressure drop evolution, and predicting the behavior of the filter.

One of the most important factor, cake area load, is measured in different ways either directly observing the weight of the filter or using other techniques. A system for continuously monitoring the weight and tension of the fabric bags was presented [3]. No information

* Corresponding author at: Institut of Chemical Engineering and Technology, University of the Punjab, Quaid-i-Azam Campus, 54590-Lahore, Pakistan. Tel.: +92 3314554867; fax: +92 4299231159.
E-mail address: msaleem.icet@pu.edu.pk (M. Saleem).

0032-5910
doi:10.1016/j.powtec.2011.08.037

on local distribution is reported. Radiometric methods were also used [4,5]. A laser displacement system was used for monitoring changes in cake height [6]. A CCD camera was used to observe and measure the increase of cake thickness with time [7]. Image from shape technique was used for measuring the cake height distributions on rigid filter media [1]. A new invasive method based on stereo vision was presented for measuring in-situ cake height on flexible filter media [8].

Surface and cloth properties influence velocity distribution and hence cake formation and detachment [9,10]. Operation at higher velocity results in compact filter cake formation [10]. An optical technique for in-situ measurement of cake height has been developed [8] and employed for the study of cake formation on needle felts [11].

Mostly, the needle felts are physically and/or chemically treated to improve their properties depending on their applications. The common surface treatment techniques are heat setting, impregnating, singeing, and calendering. Synthetic fibers are heat set to impart rigidity in the felt. Impregnating involves chemical treatment for specific requirements like acid resistant. Singeing removes extra fibers from the dust side of the needle felt. Calendering is the pressing of the felt for improved surface. Another method is applying a coating of very fine layer of an inert polymer on dust side of the needle felt. Teflon is used as membrane because of its excellent properties. The surface treatment improves dust capturing, and cake detachment on one hand while resistance to chemical attack on the other hand. The characteristics of the most commonly used needle felts are summarized elsewhere [12].

Nevertheless, to lesser or greater extent, some dust always penetrates the surface of the filter media and forms an intermediate zone which is responsible for clogging of the filter but it also helps for cake detachment. The surface layer is characterized by surface layer porosity distribution and pore size distribution [13]. Particle penetration and the dust holding capacity of different surface-treated needle felts are also important for their performance in the baghouse [14]. Operational characteristics of filter media are greatly influenced by their structure and surface properties [9,15,16].

Cake formation on heat treated and membrane coated needle felts using optical cake height measurement is investigated. Widely different needle felts 1 are intentionally selected for the purpose of comparison. Additionally the experimental rig has been designed to closely resemble the bag house. Results on evolution of pressure drop, evolution of cake height distribution, cake patches area distribution, and their characterization using fractal analysis are presented and discussed.

2. Experimental set-up

The experimental set-up consists of three rows of bags (two bags per row at maximum) enclosed in one chamber, which closely resembles a large scale bag filter equipped with necessary instrumentation for acquiring all the important data simultaneously. Operating conditions are selected in the range of commercial bag filter [12]. Sequence of bag cleaning, mode of cleaning, fraction of area to be cleaned and other parameters remain the choice of the experimenter.

2.1. The test facility

A schematic diagram of the test facility is shown in Fig. 1.

A two screw single component feeder (1) delivers a controlled constant mass (Gravimetric control, variation 1% at steady state) of powder into the dispersion nozzle (3) through a vibrating chute (2). Compressed, filtered and dried air meets the dust tangentially in the dispersion nozzle at controllable pressure up to 6 bar. Ambient air is sucked in and mixed with dispersed dust to make the dust laden gas stream. The raw gas flows through a 100 mm diameter pipe into the bag filter (4) near the bottom. The raw gas pipe is gradually expanded near the filter to reduce gas velocity before entering the filter. The separated dust settles into a dust collector at the bottom of the housing. The dust collector rests freely on a plate supported on a load cell. Both (the load cell and the dust collector (5)) are enclosed in the housing (4). The arrangement allows transient measurement of dust reaching the collector. The load cell is calibrated from 0 to 4000 ± 2 g. The range can be extended at the loss of accuracy of measurement. The gas pervades through the filter bags (6) into the clean gas header and then to the discharge fan (8).

The differential pressure regulator (3 ms time constant) monitors pressure drop across the filter. Cake detachment is accomplished on line using reverse pulse-jet. A pulse of compressed air (9) enters the bag through an 8 mm diameter hole in the gas supply pipe (27 mm diameter) tapping secondary gas from the clean gas side. One pulse is issued to each row at the upper pressure drop limit. To which row of bags the 1st jet pulse will be issued depends on the last row cleaned, however, the cyclic order is always followed unless manual cleaning is adopted. Provisions are made for three jet pulse control mechanisms. The reservoir pressure of the cleaning air can be set up to 4 bar, time of cleaning pulse can be set between 10 and 100 ms, and interval between cleaning pulses between 2 and 450 s.

The gas flow is measured using an orifice plate. The pressure drop across the orifice plate, absolute upstream pressure and temperature are recorded at 1 s resolution. The gas flow is calculated by the Lab view® software according to DIN EN-ISO5167-1: 1995 (large fan) and ISO 5167:2003 (small fan) depending on the fan in use and recorded. The gas flow measured was calibrated using Pitot tube measurements. A frequency converter is provided to regulate the gas flow.

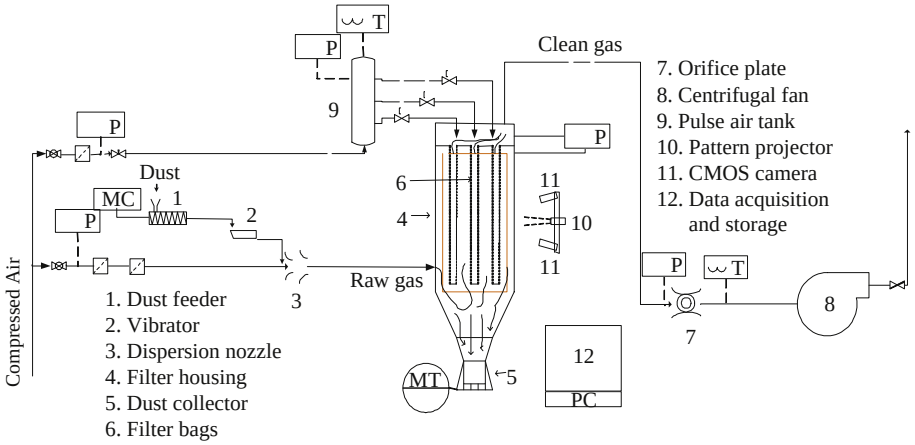

Fig. 1. A schematic diagram of the pulse-jet bag filter test facility.

Filter pressure drop (ΔP), gas temperature (T), absolute pressure (P_a), pressure in the compressed air tank (P_{jet}) and temperature (T_{jet}), dust feed rate ($\dot{m}$), and collected dust (m) are recorded along with date and time at 1 s interval. Relative humidity (H), impulse time ($\tau_{Impulse}$), interval between consecutive pulses (τ_{int}), and dispersion air pressure (P_{dis}) are recorded manually. Also the mass of dust in the feeder hopper is recorded at the start and at the end of the experiment along with the dust collector reading. Dust concentration measurements on clean gas side revealed concentrations in the range of 2–4 mg/m^3 using gravimetric methods. The overall material balance was closed at less than 1%.

Dust fraction settling in the filter and dust concentration relevant for filtration can be calculated because transient dust feed and dust collected in the filter are known. Besides an optical system is used to measure cake heights in-situ and intermittently [11].

2.2. Dust

Commercial grade non precipitated Limestone ($\rho_s = 2700$ kg/m^3) with weight mean diameter ($d_{50,3}$) of 5 μm and bulk density (ρ_b) of 1200 kg/m^3 is used as dust.

2.3. Filter media

Three types of needle felt are tested. One is made of two polymers Polyimide (PI) and Polyphenylensulfide (PPS), the second is made of single polymer Polyimide (PI) and the third one is Teflon laminated (membrane) Polyester needle felt. The first two types are heat treated on dust side. The last one is membrane coated on dust side.

The filter media are selected with two entirely different characteristics to allow comparison on two extremes of needle felts. Their mechanical properties provided by the manufacturers are summarized in Table 1. Microscopic images of the tested needle felts surface are shown in Fig. 2. The images reveal that the surface of membrane (PTFE) bags is smoother than that of the heat treated (Polyphenylensulfide (PPS) and Polyimide (PI)) needle felts.

The surface roughness of filter media is measured using a special microscope from M/s Alicona Imaging Graz, Austria. The highest and the lowest positions of the lens at which the surface is visible are manually identified. A series of images of the surface are taken while the lens traverses from the highest to the lowest position. The images are processed by the built-in software to generate a 3D surface. Different analysis can then be performed on the reconstructed digital 3D surface.

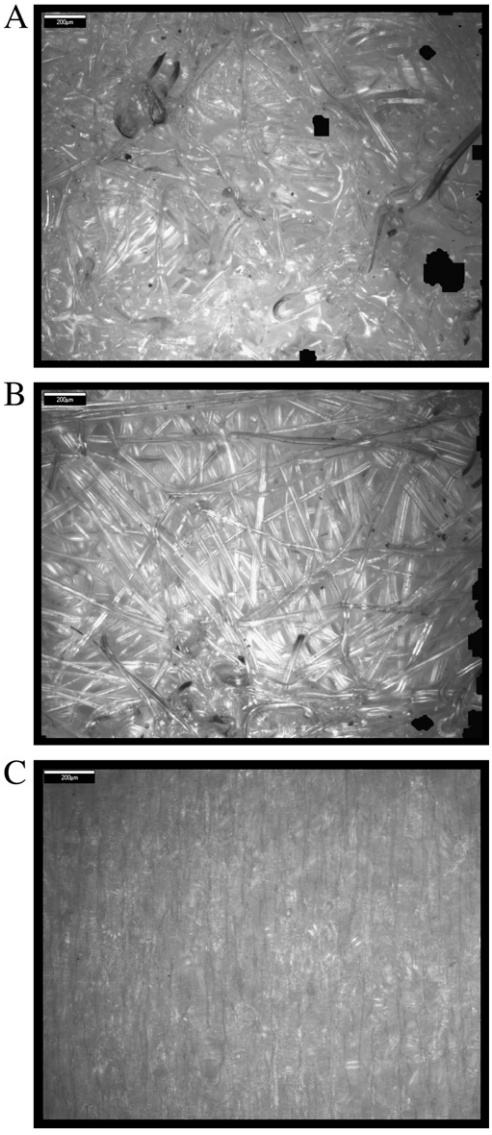

Fig. 2. Surface images of dust side of tested needle felts (A) PPS needle felt, (B) PI needle felt, and (C) Membrane coated needle felt.

Table 1
Mechanical properties of three needle felts.
Source: Company provided data sheets.

Fiber content	Polyimide (PI)+ Polyphenylenesulfide (PPS)	Polyimide+ Polyimide	PTFE laminated (Membrane) Polyester	Unit –
ID	TAN5448	TAN5446	PE	
Breaking strength, machine direction	841	743.2	601	$\frac{N}{5\ cm}$
Breaking strength, cross-machine direction	1464	2013.4	890	$\frac{N}{5\ cm}$
Strain, machine direction	27.7	29.8	–	%
Strain, cross-machine direction	35.4	48,4	–	%
Air permeability at 200 Pa ΔP	79.5	73.5	–	l/dm^2 – min
Weight	575	624	407	g/m^2
Felt construction	Supported Needlefelt	Supported Needlefelt	Supported Needlefelt	– –
Service temperature	–	–	135	deg C
Max. surge temperature	–	–	149	deg C
Thickness	–	–	1.4	mm

3. Results and discussion

3.1. Roughness of the dust side of needle felts

Roughness as distribution along a random straight line drawn on the examined surface is depicted in Fig. 3. Taking the normal surface at the median value, roughness of PI needle felt is 240–0 + 120 μm, and that of membrane needle felt is 45–0 + 20 μm. Surface roughness of heat treated needle felts is higher than that of membrane coated needle felt. Relatively deeper pores exist on PI needle felt resulting in a skewed distribution. Roughness of PPS needle felt is closer to that of PI needle felt which is not surprising because both are heat treated on dust side.

3.2. Cake formation on PPS needle felt

3.2.1. Transient pressure drop along with optical cake height measurement

An exemplary test result is displayed in Fig. 4. Here labels '*a*' and '*b*' refer to clean bag surface at different pressure drop. The labels '*c*'–'*f*' refer to cake height measurements. After the measurement marked as '*f*', the gas flow is stopped before starting jet-pulses. Stopping the gas flow at regeneration is not a normal operation but a special case adopted for the test requirement. The regeneration is actuated manually if dust cake thickness measurement is required at the end of a filtration cycle. The actuating relay circuit is opened until image acquisition by means of the optical system has been completed. After the image acquisition, the relay is closed and regeneration begins. Once the dust got settled and housing environment become clear, the gas flow and started again along with dispersion air. Cake thickness measurements after regeneration are carried out at point '*g*' at steady gas flow but no dust feed. Then the dust feed is turned on and filtration is continued for further three cycles. The positions corresponding to cake height measurements for 2nd to 4th cycles are marked using arrows without labels. The residual cake height is not measured at the start of 4th cycle.

3.2.2. Area distribution of cake height

The optical in-situ cake height measurement technique [8] is employed to study cake formation on flexible filter media.

Cake height distributions at discrete points in the filtration process are displayed in Fig. 5. Each measurement is designated by a corresponding pressure drop. The measurements around 400 Pa are at points where concave rise of pressure drop is just to change to a linear rise (Fig. 4). It can be examined that mean cake height in the first cycle is slightly higher than that in the other three cycles because corresponding pressure drop is higher (445 Pa) indicating higher cake load in the first cycle than that of the others (400 or 420). The range of cake height distribution in second to fourth cycles is apparently similar. It is obvious that pressure drop is concave at the beginning of the filtration cycle for a short time, and the dust deposited during this period is small. However, the distributions at 130 Pa (regenerated bag) and 400 Pa (end of concave rise) in the second and third cycle are only slightly different. The distributions at 400 or 420 Pa are slightly narrower than the distributions at 130 Pa on left tail indicating preferential cake formation on some area (thinner cake) than other (thicker cake) at the start of each filtration cycle after regeneration. Maximum residual cake height at 130 Pa in second and third cycles is 0.12 mm (120 μm) approximately. The measurements agree well because the residual pressure drop in both the cases is also the same (see Fig. 4). The distributions at upper pressure drop limit become narrower but the difference is not high. The mean cake height is higher in the first cycle and decreases gradually in second to fourth cycles. The slight variation is attributed to slightly different upper pressure drop and hence different cake area load at the end of respective cycles.

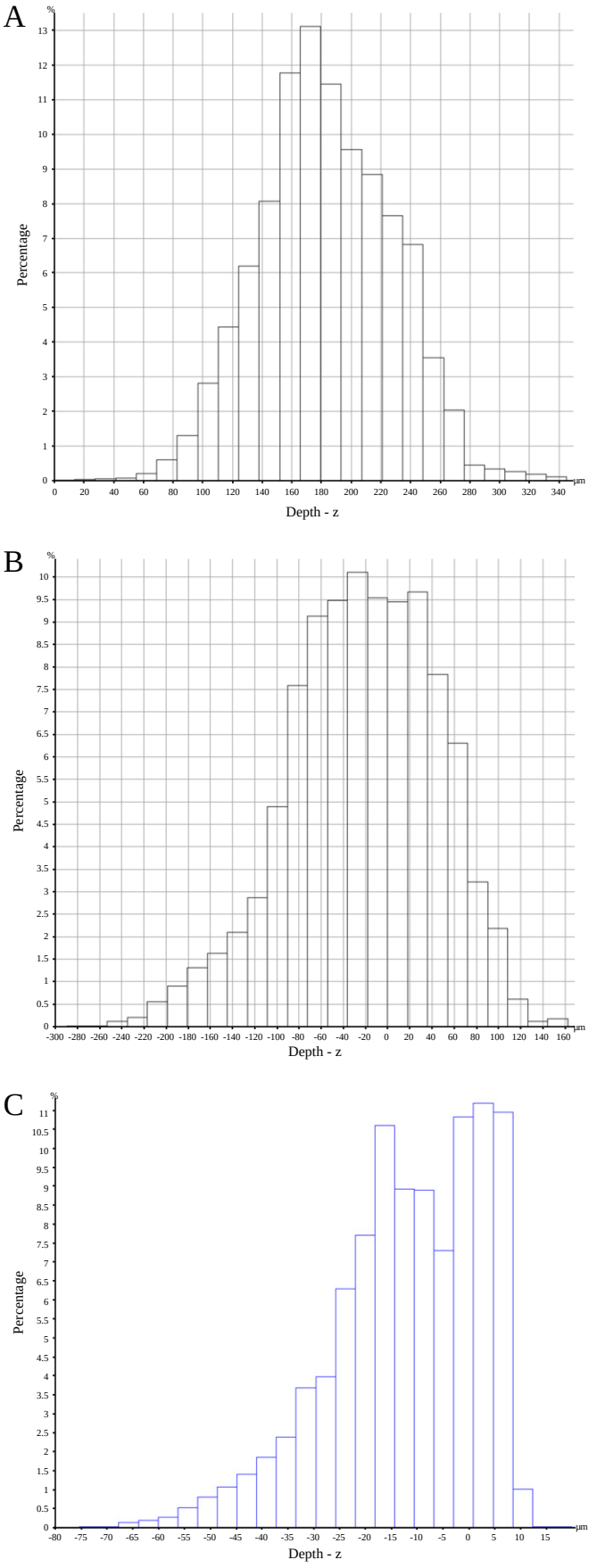

Fig. 3. Comparison of surface roughness of needle felts on dust side; (A) PPS needle felt, (B) PI needle felt, (C) Membrane coated needle felt.

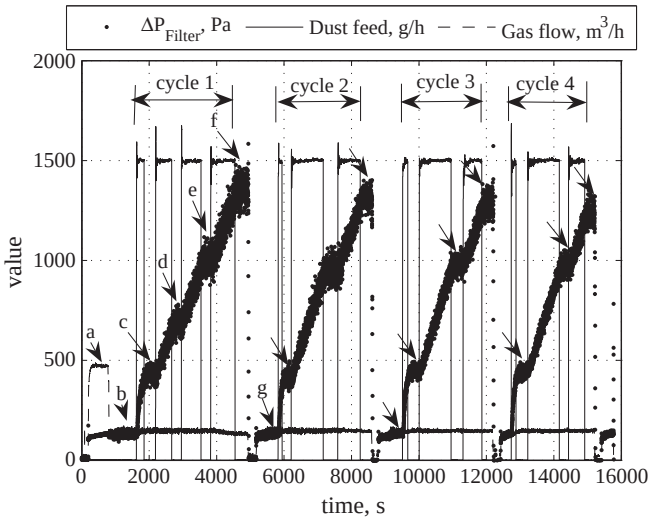

Fig. 4. Transient data of a filtration test with in-situ intermittent optical cake height measurements.

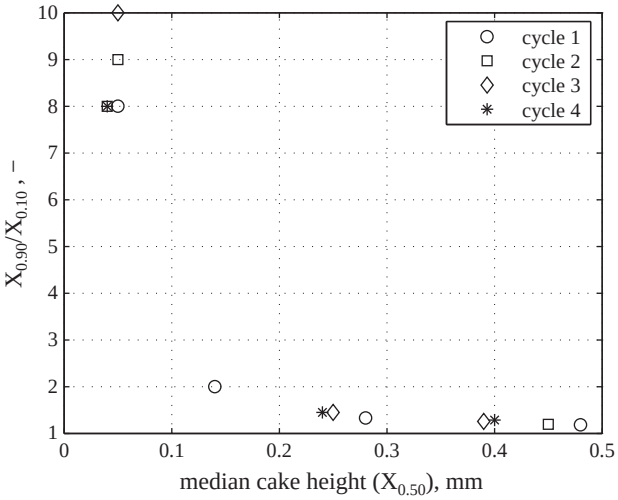

Fig. 6. Ratio of $X_{0.9}$ to $X_{0.1}$ versus $X_{0.5}$ for four filtration cycles.

Since the narrowing of height distributions is not evident from Fig. 5, the ratio of thickness at 90% area ($X_{0.90}$) to that 10% area ($X_{0.1}$) is computed. The ratio must decrease or increase depending on the narrowing or widening of the distributions. The ratio is plotted versus $X_{0.5}$ in Fig. 6 for four filtration cycles. Obviously the ratio decreases very quickly at the beginning of the filtration cycle approaching a steady value indicating that the cake height distributions become narrower on cake formation. It should be pointed out that the $X_{0.1}$ values of some measurements are zero which makes the ratio to infinity. Thus the values are taken as 0.01 mm instead of zero for some of the measurements at 130 Pa and 400 Pa.

Evolution of transient pressure drops immediately after regeneration reflects the permeability distribution of regenerated filter media. The transient pressure drop at the start of the filtration cycles (on-set of dust feed) are shown in Fig. 7. the pressure drop exhibits two distinct trends after the lag time (20–30 s) where the dust concentration relevant for filtration reaches a steady value. Initially a concave rise followed by a linear rise during the cycle. The concave part is shorter

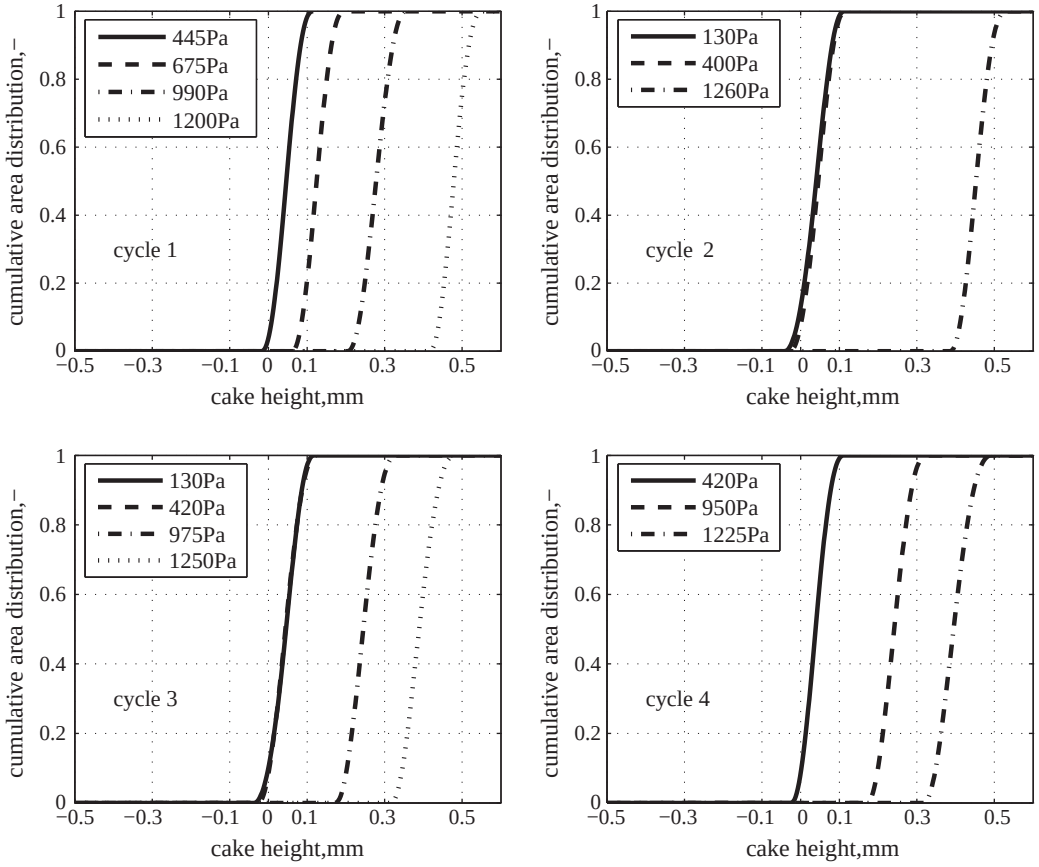

Fig. 5. Cumulative area distribution of cake height during filtration cycles. The test conditions are: $u = 20.7$ mm/s, $c = 7.17$ g/m^3, $P_{jet} = 3.6$ bar, and $H = 55\%$ at 27 °C.

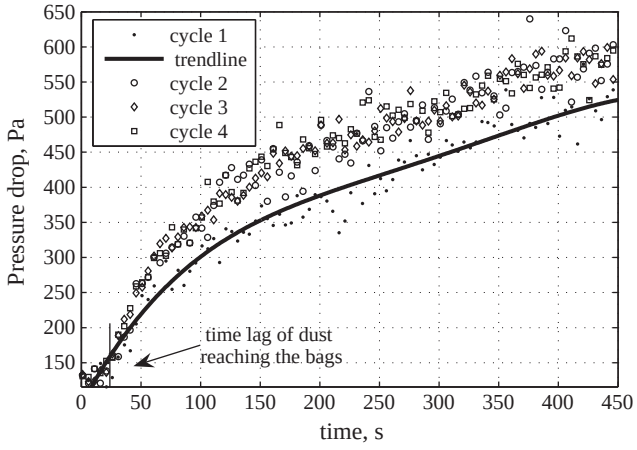

Fig. 7. Transient pressure drop across the filter.

(150 s) as compared to the overall cycle time. A gradual transition from concave to linear rise can be observed in all cases.

The pressure drop across the filter is normally taken as the sum of two contributions [12], one of the filter media, and the second of the deposited cake. Starting at thoroughly pulsed filter bags, the pressure drop should be increasing linearly on filtration expecting a uniform cake on the filter surface possessing uniform specific cake resistance. There is a distribution of residual cake on the bags after regeneration at the upper pressure drop limit. The distribution of cake is because of either a fraction of total area being regenerated or incomplete cake detachment. The pressure drop evolution following regeneration, therefore, depends on how the local filtration velocity (u), cake area load (w) and cake resistance (k_c) vary over time. Concave rise of pressure drop may result under different scenarios:

- A fraction of total filter area is pulsed at the end of a filtration cycle although cake detachment from regenerated area is complete. After regeneration some areas hold no cake while others hold residual cake. On resuming filtration, the gas flow is higher through the areas holding no cake as compared to the areas holding thick cake at the same overall pressure drop. The rate of increase of cake height can be taken proportional to the velocity at constant dust concentration ($dw/dt = c.u$) provided the cake is incompressible. In such a case, the cake height will increases faster at regenerated areas than the residual cake laden areas. Thus pressure drop may increase faster at the beginning. As the regenerated areas get a layer of cake thicker and thicker, eventually, a point is reached where the overall resistance to flow is equilibrated across the bags. From this point onwards the velocity is uniform and a linear pressure drop rise is observed.
- A concave rise may also be observed when all bags are pulsed but the cake detachment is incomplete, i.e. patchy cleaning prevails.
- A concave rise might also be observed if the local dust concentration is increased due to disintegrated cake on pulse cleaning according to $dw/dt = c.u$ at constant u. More dust reaches the bag in very short time immediately after regeneration leading to faster increase of cake height. These phenomena should not last more than the lag time (ratio of the hold volume to the gas volume flow $\approx$20 s).
- A concave rise may also be observed merely due to a permeability distribution of filter media. The pore blocking takes place on filtration. The pressure drop rise is concave until a particle-fiber layer is formed prior to a true surface filtration. A typical phenomenon with heat treated filter media as reported in literature [13].

At low mechanical stability cake compaction is considered as one of the reasons for non-linear i.e. convex pressure drop rise which results in shorter cleaning intervals [17]. A concave pressure drop rise shortly after regeneration followed by a linear rise is often related to particle re-entrainment and/or patchy cleaning [18]. Patchy cleaning results in a locally higher filtration velocity leading to a faster build-up of filter cake in the regenerated areas [19]. Also patchy cleaning results in a concave rise of the overall pressure drop when only a fraction of total filter area is cleaned at the end of filtration cycle which is pointed out and simulated by [19].

In the presented case (Fig. 7), all bags are regenerated off-line at the upper pressure drop limit. Therefore, there is no fraction of jet pulsed area. Reattachment or increased dust concentration are excluded as well since the gas flow is stopped during jet pulse cleaning. Therefore, none of the fractional cleaning, reattachment, or increased dust concentration, is responsible for the observed concave rise of pressure drop. Then permeability distribution of the filter media and filter cake are responsible for concave rise of the pressure drop. Comparing pressure drop curves Fig. 7, one can conclude that concavity in the first cycle is due to permeability distribution of the filter media alone. The residual cake in the subsequent cycles enhances the concavity of pressure drop curves.

The naked eye examination revealed that the cleaning conditions are such that the cake is detached leaving behind only a thin layer. The residual layer is observed as comprised of a large number of small cake structures. Equivalent diameter $(4 \cdot A/\pi)^{0.5}$ computed from optically measured residual cake patch size analysis reveals that the bag surface is mostly covered with a thin layer of dust along with small fragments in the size range of 1–5 mm (see Fig. 8). The cake height measurements reveal that the maximum height of residual cake is less than 120 μm.

Based on pressure drop evolution, one expects a narrow cake height distribution on cake formation. The cake height distribution at 400 Pa is narrower than the one at 130 Pa in cycle 3 in Fig. 5. The same is true for the measurements at the end of the cycles. Once a certain dust mass has initially deposited on the surface of the filter which initially had a distribution of resistance, the formed cake may possess different characteristics (e.g. specific cake resistance and porosity). Thus the overall resistance offered by filter media and the filter cake to the gas flow is equilibrated. The gas flow and the cake growth become uniform leading to linear pressure drop rise. The monotonically increasing rate of cake growth is supported by the linear rise of pressure drop.

Provided the gas flow is distributed non-uniformly at the filter surface after regeneration, a cake of higher resistance should be formed at the start of filtration [9,10]. Resistance of the filter cake should decrease gradually as the flow distribution becomes uniform. Since transient mass input and collected mass are known and clean

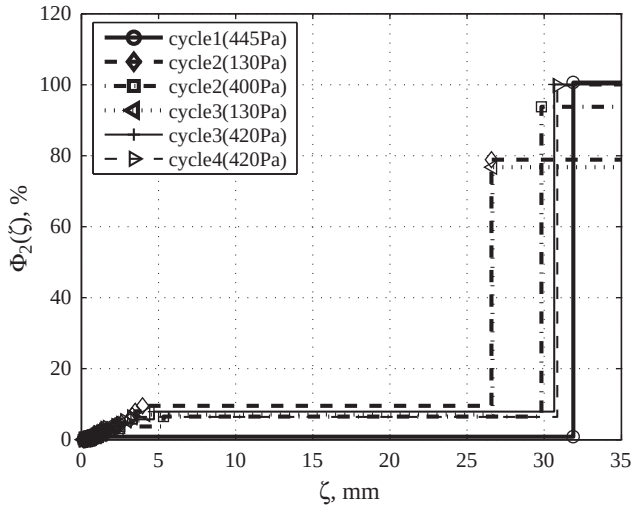

Fig. 8. Cumulative cake patch area versus equivalent diameter. The test is performed at $u = 20.7$ mm/s, $c = 7.17$ g/m^3, $P_{jet} = 3.6$ bar, and $H = 55\%$ at 27 °C.

gas dust concentration is negligible, the material balance allows to compute transient cake areal load and hence the specific resistance of the forming cake. The specific cake resistance is calculated from the slope of the pressure drop curve averaged over time (Δt), cake area load (w, g/m^2), filtration velocity (u, m/s), viscosity (μ, Pa.s), and filtration area (A, m^2), according to Darcy's law and represents the mean value over the interval Δt (time interval of dust feeding between two consecutive cake height measurements).

Specific resistance of filter cake (k_c, m/kg) is plotted versus cake area load (w) in Fig. 9. The cake area load is calculated from the corrected duct concentration (c_{cor}, g/m^3), gas flow rate (V, m^3/s) and filtration time (t_f, s). The resistance is higher at the beginning of the filtration cycle and lower otherwise. The cake area load decreases from 300 g/m^2 at the end of the first cycle to 230 g/m^2 at the end off fourth cycle. The decreased cake area load at the end of cycle from first to the second cycle is more pronounced as compared to the second, third or fourth. Since the gas flow and the dust concentration are about constant, the change of the dust load is due to reduced filtration time which may be associated with the reduced filter permeability. The residual pressure drop (ΔP_{res}) at the start of each filtration cycle is found in the range of 130 ± 5 Pa which indicates that the residual permeability of the bags is not changed although small amount of the residual cake is distributed on the surface. Thus the higher ΔP for the same dust area load (w) in second to fourth cycles as compared to first cycle (see Fig. 7) is due to the modified cake characteristic which is formed on the regenerated surface possibly under locally differing flow conditions. The analysis revealed that the transition of the pressure drop curve took place at nearly 250 Pa in the first cycle whereas the transition is observed at nearly 350 ± 20 Pa in the second to fourth cycles. This transition took place although the time until this transition occurred in the range of 70 ± 10 s including the lag time (hold volume of the filter housing/gas volume flow rate) which is constant at approximately 20 s. Thus a difference of nearly 100 Pa exists at nearly the same cake area load. The reduction of cycle time might be attributed to a high resistance of the initial layers of forming cake, since the specific cake resistance after the initial transition cake formation phase remains nearly constant (see Fig. 9). As a result the pressure drop rises faster and the time of filtration is reduced from second to fourth filtration cycles at nearly the same upper and lower pressure drop limits.

3.2.3. Area distribution of cake patches

Filter cake which is not detached is called 'cake patch' where as a cake free area is termed as 'clean patch'. The cumulative area of cake patches (percent of measured area) is plotted against the equivalent diameter of the cake patches for 6 measurements in Fig. 8. The patches area equals the number of pixels in each object multiplied by area per pixel. The equivalent diameter is the diameter of a circle being area equivalent to the cake patch. Retrieved data is then transformed to a cumulative percent area. The identified patches and respective equivalent diameters are sorted according to the size. Area of each patch is divided by the total area of the analyzed section and then added to get a cumulative sum of patches area. The equivalent diameter is converted from pixels to mm by using the conversion factor of 0.1 mm/pixel (based on image resolution).

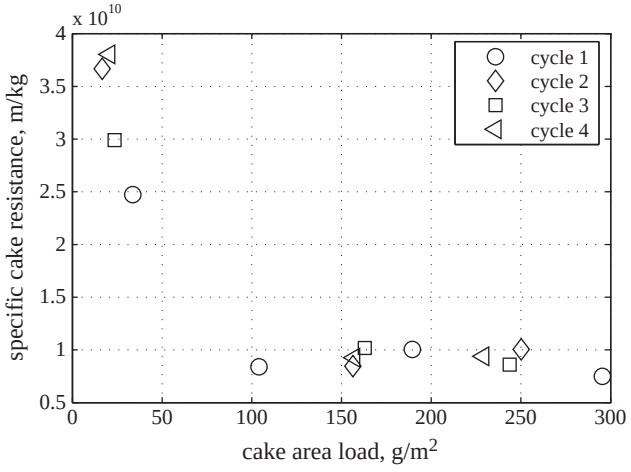

Fig. 9. Specific cake resistance of limestone dust cake. The test is performed at $u = 20.7$ mm/s, $c = 7.17$ g/m^3, $P_{jet} = 3.6$ bar, and $H = 55\%$ at 27 °C.

The data for regenerated bag and at the end of concave rise of pressure drop is presented as the cake formation following regeneration is of interest. As soon as the pressure drop rise becomes linear, almost 99% bag surface is dust covered. Residual cake patches area makes up to approximately 75% of the total area after first regeneration. A large cake patch and many small cake patches are identified. The size of the cake patches increases as the filtration continues. One large cake patch grows up to approximately 90% of the total area. The smaller cake patches gradually merge depending on their size and distribution. However, in all measurements above 445 Pa only one cake patch is identified (those measurements are not shown here as there is only one patch of 100% cake area). Disappearance of smaller patches and increasing size of larger cake patches indicates the preferred lateral dust deposition on the boundary.

Assuming preferential dust deposition on clean patches following regeneration, one should not see any clean patches after the bags have been exposed to dust laden gas for more than 150 s. However, one observes a gradual reduction of the clean patches and an increasing size of larger cake patches over this time period (nearly 150–250 s). A small number of clean patches are still identified at 445, 400 or 420 Pa as can be seen in Fig. 8. Therefore, the hypothesis that the cake formation following regeneration is merely on clean patches seems not absolutely true. It is plausible to consider that the cake patches grow faster in lateral direction at the bottom and in a short time the clean patches disappear although the cake height has not been equalized everywhere. An evidence to this observation was obtained in a separate test as shown in Fig. 10 where cake height of newly formed cake and survived cake from previous regeneration has not equalized 10 min from the start of dust feed. Therefore, the cake forming on regenerated areas should be compact than the cake forming on top of the survived cake patches from previous regeneration because of different local velocity.

The comparison of cake height distributions of regenerated (130 Pa) and dust laden bag (400–445 Pa) in Fig. 5 revealed that the maximum cake height on the regenerated bag and the dust laden bag does not increase significantly unless the cake patch area approaches 100% (Fig. 8).

Pressure drop across the filter is usually assumed to be a sum of pressure drops due to filter media and filter cake. The pressure drop is calculated using Darcy's Law applicable to laminar flow through porous bed of solids. Usually a one dimensional flow is assumed. The pressure drop is computed at an area averaged filtration velocity and average resistance is assumed. The situation is an over simplification of the ground reality. It is not necessary that the whole regenerated filter surface will become free of dust [1,2]. A two dimensional flow model was applied to describe the pressure drop evolution on patchily regenerated filter surface. It is considered that the cake formation on boundary of cake patches grows faster in lateral direction. In short time the clean patches are covered with initial layer of dust of higher specific resistance after which cake growth at the patches boundary is two dimensional. Filter cake grow laterally (size) and vertically (height).

3.2.4. Characterization of cake patches boundary

The fractal dimension (D) provides a means to characterize complex systems like dust cake structure and the cake patches [20] which had been employed for the characterization of dendrites formed by

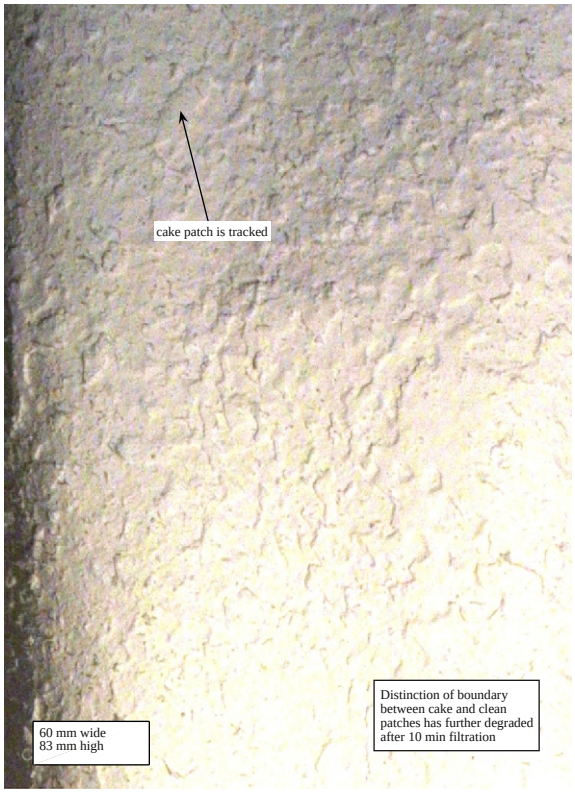

Fig. 10. An image of a filter/cake surface after 10 min of filtration following regeneration. Height difference of new and survived cake has decreased. Old cake patches boundary has smeared out but old patches can be identified.

the collection of particles on fibers [21]. The box-counting dimension (D) is defined as $D = \log(N)/\log(r)$ where N is the number of boxes of side length r covering the fractal object and D is the box dimension.

It is convenient to use available image processing tools to calculate the box-counting dimension on a very large number of images. A grid with a side length of each grid element r = 1/(width of grid) is defined and overlaid on the object image. Then the number of boxes of the grid that contain any part of the object is counted as N(r). The same process is repeated with a new grid size. The grid size changes from 2 to 315 pixels in 30 steps. The grid is subjected to 1000 random offsets. The computations are performed to get an average value of box counts for a single grid size. Then a plot of log (N) versus log(r) is generated. The slope of the linear fit of the data points leads to the box counting dimension (D).

A complex boundary will possess higher fractal dimension and vice versa. The cake patches boundary will modify on cake formation following regeneration. The optical cake height measurements have shown the existence of cake height distribution on the surface. The patch size analysis revealed that cake patches of various sizes exist on the surface and grow in size and height on commencement of filtration.

The fractal dimension (D) is computed after applying a threshold which expresses the patch boundaries (equivalent to slicing of cake surface and looking at the edges). The threshold is varied within the range of present cake height. The variation of the batch boundary at different positions from the bag surface reveals the uniformity of the cake height. The fractal dimension of two measurements for residual cake patches (130 Pa), two measurements of formed cake immediately after regeneration (400 and 420 Pa), and two measurements at the end of filtration cycle (1200 and 1260 Pa) are shown in Fig. 11 versus the threshold (cake height, mm). The fractal dimension of residual patches is around 1.35 at bottom (zero threshold) which increases to a maximum (1.45) at 0.05 mm threshold and declines again. This observation indicates that the boundary of residual cake is complex midway between the bottom and top of the cake patches. It also indicates that the residual cake height is in the range of zero to 0.1 mm. The measurements corresponding to 400 Pa and 420 Pa correspond to the point where concave rise disappears and a linear rise of pressure drop begins. The fractal dimension increases away from the base of the cake and reaches a maximum value while the cake heights are in the same range. Over this interval the maximum cake height does not changes although fractal dimension at the top of the cake slightly increases. Increase in fractal dimension indicates enhanced complexity of the patches boundary at the top. No increase in maximum cake height reflects upon preferential dust deposition on regenerated areas. Slight decrease in fractal dimension at the base of the cake at 400 Pa and 420 Pa also supports deposition of dust on regenerated areas. Thus immediately after regeneration, the dust deposition on regenerated areas could be concluded besides modified cake boundaries away from the base. The modified boundary could be attributed to relocation of dust as well as deposition of small amounts of dust. This gives rise to the hypothesis that cake growth at boundary occurs simultaneously in lateral as well as vertical directions contrary to lateral only. If it is believed that the dust deposits only on the clean patches preferably, then shortly after regeneration the clean patches

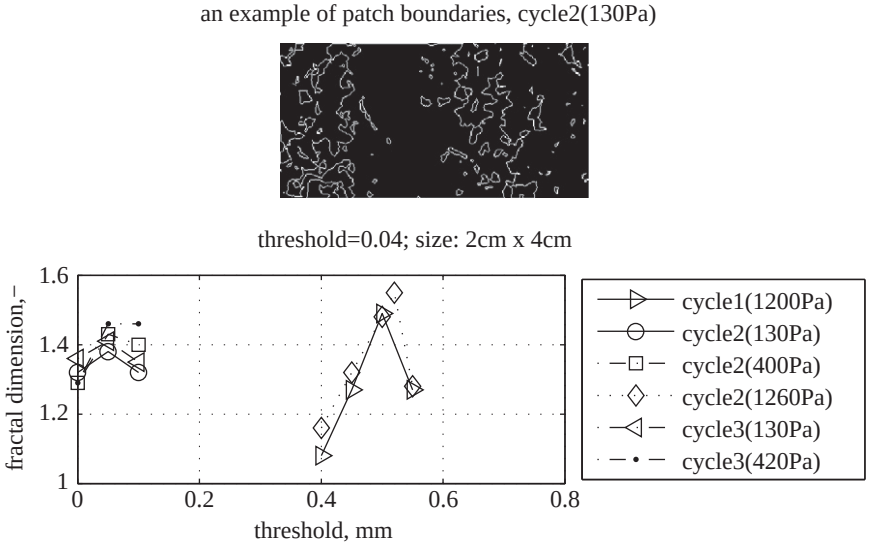

Fig. 11. Characterization of cake patches boundary using fractal analysis.

should have disappeared and fractal dimension of the cake patches boundary must have reduced to one.

3.3. Cake formation on PI needle felt

3.3.1. Transient pressure drop along with optical cake height measurement

Filter bags are conditioned prior to the filtration test. The pressure drop curve during the filtration test is shown in Fig. 12 along with discontinuous in-situ cake height measurements for two filtration cycles. First cycle starts with completely pulsed bags. The second cycle starts with one third filter area being pulse-jet cleaned. Dust feed is cut-off for cake height measurement while air flow is kept on. Labels 'a' to 'i' in Fig. 12 refer to cake height measurements. Dust feed rate and air flow rate are also displayed.

It is obvious from Fig. 12 that pressure drop evolution is steeper at the start of the first cycle. A similar trend is observed in the second case where one third of filter area is subjected to jet pulses. The pressure drop becomes moderate and linear following a short transition in the first cycle whereas it continuously declines in the other case of partial cleaning till the end of the cycle. This trend reflects upon a strong influence of non-uniform cake area load on pressure drop evolution resulting from partial cleaning. The steep rise in the first cycle is solely from the filter media itself while it is attributed to patchy cleaning in the second case. A similar behavior is observed with PPS needle felt in Section 3.2.1.

Cake height distributions at different operating pressure drops are shown in Fig. 13. The height distributions at 275 Pa, 462 Pa, 660 Pa, 800 Pa, 1015 Pa, and 1200 Pa are displayed. The photosensitive nature of PI fibers affects the visibility of black and white projected patters and creates problems in reconstruction of the surface. Since the magnitude of error cannot be quantified due to the, problems with black and white pattern recognition on the surface and subsequently with the surface reconstruction, the measurements are erroneous but they capture the trend of cake formation. This is one of the limitations of the optical technique employed in this study.

3.3.2. Cake patches area distributions

Owing to error in optical measurements, cake patch size analysis is meaningless.

3.4. Cake formation on PTFE laminated polyester needle felt

3.4.1. Transient pressure drop along with cake height measurements

Fig. 14 shows data from a filtration test with conditioned bags for a single cycle with intermittent cake height measurement. Simultaneously

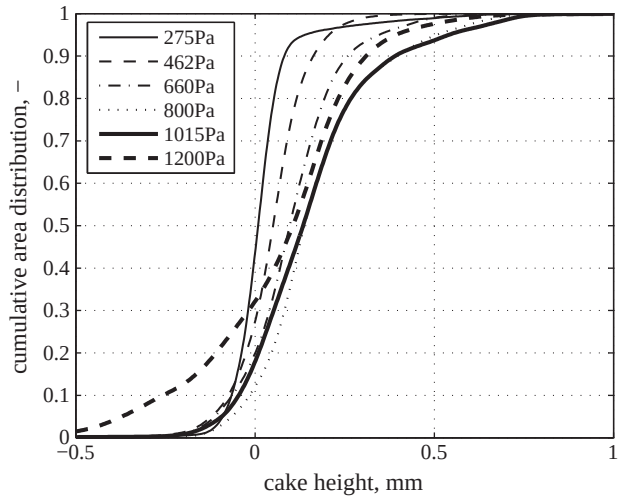

Fig. 13. Evolution of area distribution of cake height on PI bags at 27.3 mm/s and 4.33 g/m^3 on thoroughly regenerated bags.

measured dust rate (*g*/h), gas rate (m^3/h), collected dust (*g*) and pressure drop (Pa) are displayed.

The pressure drop in Fig. 14 is linear as expected. No concave rise in pressure drop is observed on the cake formation on thoroughly jet pulsed membrane coated needle felt at the start of filtration contrary to that on heat treated needle felts (PPS and PI needle felts).

The pressure drop rise is linear during filtration periods, however, after 1000 Pa the curve shows convex rise and sudden jumps as shown in Fig. 14. Different factors might be considered responsible, for example, increased dust concentration, increased local velocity, increased density of the cake due to compaction or dilution effect from chamber air mixing. High dust concentration can be excluded because dust feed and gas flow are well regulated to assume constant dust concentration. Since filtration starts on thoroughly jet pulsed bags with uniform cake formation, thus increased velocity is not appropriate reason. With the on-set of dust feed, air in the chamber is mixed with the incoming dust laden gas giving rise to relatively low concentration. Dust concentration gradually increases to reach its steady value and therefore pressure drop rise is convex. Further, on uniform and thoroughly cleaned surface, the cake formed is fragile and possesses low mechanical strength. As cake thickness increases, pressure drop across the cake and hence the force increases which causes compaction of the cake near 1000 Pa and above. Such behavior

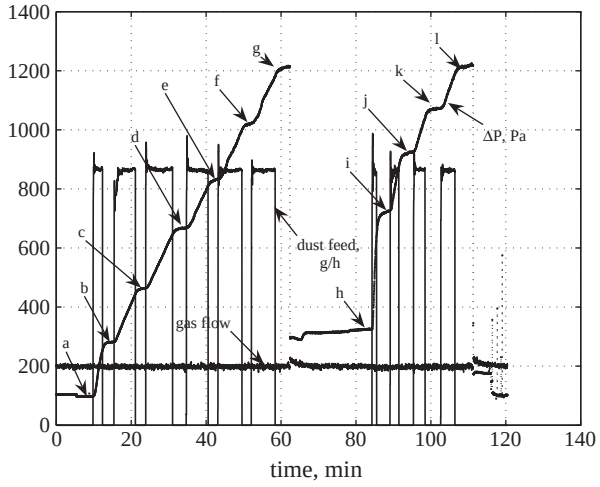

Fig. 12. Transient data of pressure drop, dust feed rate, and gas flow from two filtration cycles using bags made of heat treated Polyimide (PI) needle felt.

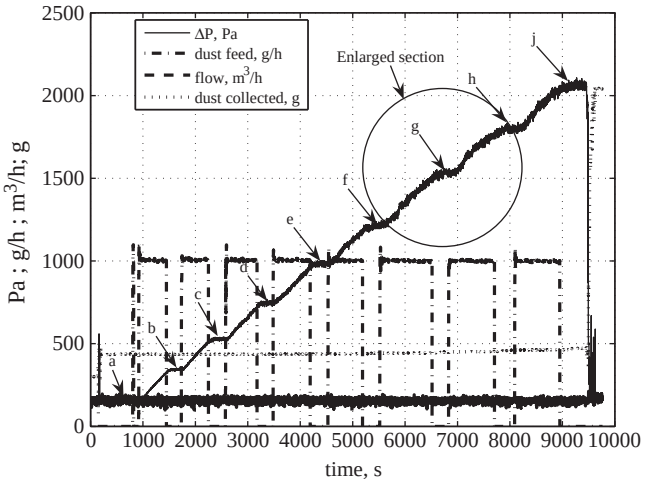

Fig. 14. Cake formation with intermittent cake height distribution measurement on membrane coated needle felt.

has already been observed with cake formation on PPS [11]. Cake compaction has also been reported [22].

Cumulative area distributions of cake heights at respective pressure drops are shown in Fig. 15. All measurements are relative to thoroughly jet pulsed bag surface at point 'a' in Fig. 14. At point 'a' two measurements are taken. The curve at 145 Pa is a relative measurement of the same surface. Measurements at 340 Pa and 530 Pa show a cake on most of the surface and are shifted rightwards. After 530 Pa, with the increase in mean cake height, the area distributions become wider. The measurement at 530 Pa indicates a uniform distribution of cake height between 0.12 and 0.25 mm. The measurement at 983 Pa indicates a bi-modality at point (a). The measurement at 1204 Pa shows two modes (b1 and b2). Although the cake height cannot be judged from visual examination, however, a smooth cake surface is observed with the naked eye. The only explanation to the widening of distributions on cake formation, especially above 1000 Pa, can be based on local compaction of the filter cake which is reflected by the pressure drop curve in Fig. 14. It appears that local compaction occurs at 1000 Pa and above which causes widening of cake height distribution captured by the optical system. From the cake height measurements and the pressure drop observations it can be stated that at relatively low filtration velocity (20.7 mm/s) and uniform permeability distribution leads to the formation of uniform and fragile cake. As the cake thickness increases, the pressure drop and hence the compression force on the cake also increases. At certain points, 1000 Pa and above, the pressure drop across the cake causes mechanical failure of the cake, thereby, the cake compacts only at some locations. Resultantly the flow distribution and hence pressure drop is disturbed until the flow is uniformly distributed again. Hence the cake compaction generates different cake heights and subsequently wider and multi-modal cake height area distribution. It is obvious that the pressure drop at which local compaction may take place depends upon the conditions of cake formation. Compaction of filter cake at higher pressure drop is also reported in literature [17].

3.4.2. Cake patches area distribution

Results for completely pulse jet cleaned and patchily cleaned filter bags are presented in Fig. 16. First measurement in Fig. 16-A is at 340 Pa, shortly after starting dust feed, while the first measurement in Fig. 16-B is immediately after regeneration.

The plot of cumulative cake patches area $\Phi_2(\zeta)$ versus equivalent diameter of cake patches(ζ) in Fig. 16-(A) shows few patches of less than 3 mm and one patch of nearly 27 mm. Cumulative area is almost

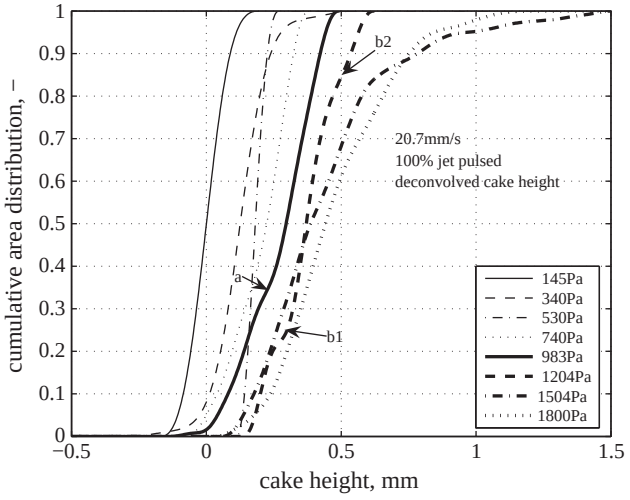

Fig. 15. Cumulative area distribution of cake height during cake formation on thoroughly regenerated membrane coated needle felt at $u = 20.7$ mm/s and $P_{jet} = 4$ bar.

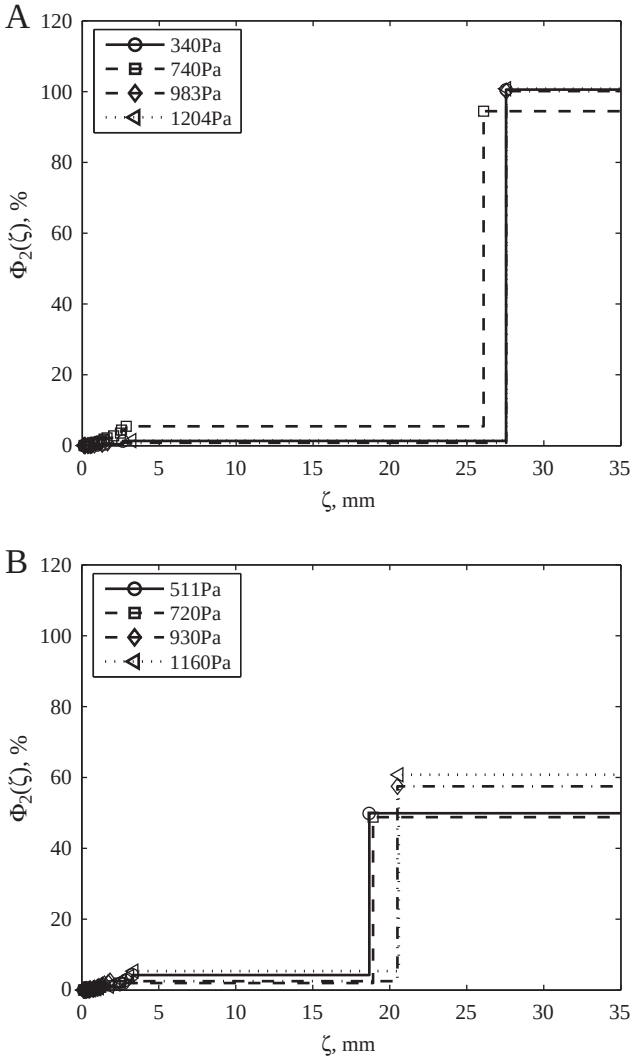

Fig. 16. Cumulative area of cake patches versus equivalent diameter on membrane coated needle felt: (A) when all bags are jet pulsed at $u = 20.7$ mm/s and $P_{jet} = 4$ bar and (B) when 33% area is jet pulsed at $u = 20.7$ mm/s and $P_{jet} = 1.7$ bar.

100% which agrees well with the expectation. On patchily regenerated surface in Fig. 16-(B), few small patches of less than 4 mm and one large patch of 17 mm are identified at 511 Pa. Nearly 50% surface is dust free. On cake formation, at 720 Pa, patches size does not change, while only few small patches disappear. At 930 Pa and 1160 Pa, mainly the large patches grow. The cumulative cake patches area increases from 50% to 60%. Nearly 40% area is dust free which is in contradiction to the pressure drop rise. Despite this contradiction a thin cake can be supposed on 40% area and thicker cake on the rest. Thicker cake patches area increases by 10% indicating a two dimensional cake formation on the boundary of patches. Increasing mean cake height and right shifting cake height distributions support this argument.

The presented patch size analysis is based on zero threshold cake height which reveals the cake formation at the base of the patches. The cake formation on edges of cake patches can be observed if threshold is varied over the expected cake height. Fig. 17 presents the arithmetic mean equivalent diameter (MED) of cake patches at various thresholds of regenerated and the next cake formation at 20.7 mm/s. The MED varies from 17 mm to 2 mm over 0 mm to 0.35 mm threshold on regenerated needle felt. It means that there is no cake above 0.3 mm. On cake formation MED at zero threshold rises from 17 mm to 35 mm indicating fully dust covered needle felt. At 0.05 mm threshold, MED is 22 mm, which may be due to few small patches along with one large patch making arithmetic

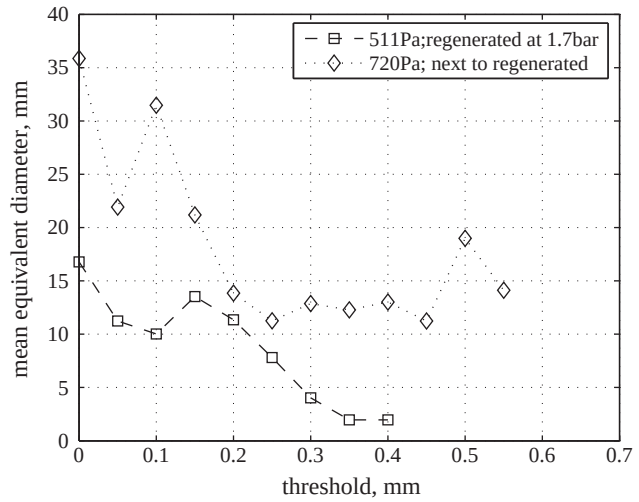

Fig. 17. Variation of mean equivalent diameter of cake patches versus threshold cake height on membrane coated needle felt at $u = 20.7$ mm/s.

mean smaller. Thus MED reaches a steady value of nearly 13 mm over 0.2 mm to 0.45 mm. On cake formation maximum cake is in this height range.

3.4.3. Characterization of patches boundary using fractal dimension (FD)

Computed fractal dimension (D) of cake patches boundary are plotted versus threshold cake height in Fig. 18 for residual cake patches on patchily regenerated bags (511 Pa) and formed cake on patchily regenerated bags at (720 Pa). Data depicts that fractal dimension slightly increases and then decreases quickly with threshold at 511 Pa at 20.7 mm/s. The fractal dimension reaches a limiting value beyond 0.2 mm threshold. At 720 Pa, fractal dimension has significantly decreased indicating smoother patches boundary (edges smear out). A limiting value is reached after 0.2 mm threshold where fractal dimension is slightly higher than 1 (BD of a smooth line or a bounding box). The analysis shows that patches grow and edges smear out on cake formation immediately after regeneration. Fractal dimension of filter cake fragment is also reported around 1.6 in the literature [23]. Maximum cake height has not changed significantly over 511 Pa–720 Pa, however, cake height at the base increases indicated by modified fractal dimension at the base.

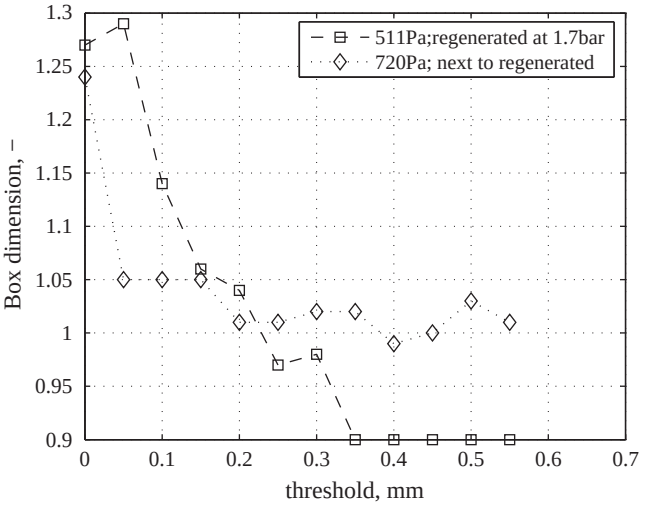

Fig. 18. Variation of box dimension with threshold cake height at $u = 20.7$ mm/s on membrane coated needle felt.

4. Conclusions

Cake formation studies with heat treated and membrane coated needle felts in pilot scale pulse jet bag filter were carried out. Pressure drop evolution, cake height distributions, cake patches area distribution and their characterization using fractal analysis are presented.

Pressure drop evolution during cake formation for partially pulsed filter bags is concave irrespective of filter media. However, heat treated filter media give rise to concave pressure drop evolution even with fully cleaned filter bags. Permeability distribution of filter media either due to its structure or in-homogeneously distributed cake is primarily responsible for concave evolution of filter pressure drop. Thus filter media does play a role in cake formation. A strong influence of the distribution of filter cake is obvious.

Patchy cleaning is observed only when jet pulse pressure is too low and unable to provide necessary force for cake detachment. Due to variation in dust and filter media properties, it is not possible at this stage to define a general limit as a criteria for cake detachment. However, based on experiments with limestone dust and three types of filter media, it can be suggested with confidence that cake will be completely detached at pulse pressure above 4 bar and filtration velocity below 50 mm/s except a thin residual layer (100–200 μm). The uniformity of residual layer depends on the surface characteristics of the filter media.

Patch size analysis and fractal analysis reveal that residual cake grow in size following regeneration initially on the base with edges smearing out. The height difference is not leveled off which indicates the existence of cakes with different densities due to different conditions locally.

Cake height measurements with PI needle felts were hampered on account of its photosensitive nature. Therefore, the developed technique cannot be used for cake height measurements on photosensitive filter media.

Acknowledgments

Authors acknowledge the project funding by Austrian Science Foundation (FWF) under project P 16313-No.7, financial support from Higher Education Commission, Islamabad, Pakistan, supply of needle felts by M/S Inspec Fibers (Lenzing, Austria), and M/S Alicona Imaging (Graz, Austria) for microscopic analysis of needle felts.

References

[1] A. Dittler, B. Gutman, R. Lichtenberger, H. Weber, G. Kasper, Optical in situ measurement of dust cake thickness distributions on rigid filter media for gas cleaning, Powder Technology 99 (2) (1998) 177–184.
[2] H. Leubner, U. Riebel, Pulse jet cleaning of textile and rigid filter media-characteristic parameters, Chemical Engineering and Technology 27 (6) (2004) 652–661.
[3] J.A. Cross, R. Helstroom, R. Beck, Method for continuously monitoring the weight and tension of filter bags in a fabric filter system, Filtration and Separation 32 (5) (1995) 443–447.
[4] R. Klingel, Untersuchung der Partikelabscheidung aus Gasen an einem Schlauchfilter mit Druckstossabreinigung, 76, Verein Deutscher Ingenieure(VDI)-Verlag GmbH, Düsseldorf, 1983.
[5] C.R. Holland, Build-up and release of dust cakes on felted filter fabrics, Filtration and Separation (1986) 372–376.
[6] Y.H. Cheng, C.J. Tsai, Factors influencing pressure drop through a dust cake during filtration, Aerosol Science and Technology 29 (1998) 315–328.
[7] Y. Endo, D.R. Chen, D.Y.H. Pui, Effects of particle polydispersity and shape factor during dust cake loading on air filters, Powder Technology 98 (3) (1998) 241–249.
[8] M. Rüther, M. Saleem, H. Bischof, G. Krammer, In-situ measurement of dust deposition on bag filters using stereo vision and non-rigid registration, Assembly Automation 25 (3) (2005) 196–203.
[9] K.T. Hindy, J. Sievert, F. Löffler, Influence of cloth structure on operational characteristics of pulse-jet cleaned filter bags, Environment International 13 (2) (1987) 175–181.
[10] C.C. Chen, W.Y. Chen, S.H. Huang, W.Y. Lin, Y. Kuo, F.T. Jeng, Experimental study on the loading characteristics of needle felt filters with micrometer-sized monodisperse aerosols, Aerosol Science and Technology 34 (2001) 262–273.

[11] M. Saleem, G. Krammer, Optical in-situ measurement of filter cake height during bag filter plant operation, Powder Technology 173 (2007) 93–106.
[12] F. Löffler, H. Dietrich, W. Flatt, Dust collection with bag and envelop filters, Fried Vieweg and Sons, Braunschweig, Germany, 1988.
[13] W. Höflinger, G. Mauschitz, W. Koschutnig, Cleaning behaviour of textile filter media, European Conference on Filtration and Separation, Gotenberg-Germany, 2002.
[14] W. Hoeflinger, H. Rud, G. Mauschitz, Estimation of the particle penetration and the dust holding capacity of different surface-treated needle felts, Separation and Purification Technology 58 (2) (2007) 256–261.
[15] E. Tanabe, P. Barros, K. Rodrigues, M. Aguiar, Experimental investigation of deposition and removal of particles during gas filtration with various fabric filters, Separation and Purification Technology 80 (2) (2011) 187–195.
[16] D. Jiang, W. Zhang, J. Liu, W. Geng, Z. Ren, Filtration and regeneration behavior of polytetrafluoroethylene membrane for dusty gas treatment, Korean Journal of Chemical Engineering 25 (2008) 744–753, doi:10.1007/s11814-008-0122-2 http://dx.doi.org/10.1007/s11814-008-0122-2.
[17] E. Schmidt, Experimental investigations into the compression of dust cakes deposited on filter media, Filtration and Separation 32 (8) (1995) 789–793.
[18] D.H. Smith, V. Powell, G. Ahmadi, E. Ibrahim, Analysis of operational filtration data part I. ideal candle filter behaviour, Powder Technology 94 (1997) 15–21.
[19] A. Kavouras, G. Krammer, Deriving cake detachment versus cake area load in a jet pulsed filter by a mechanistic model, Powder Technology 133 (2003) 134–146.
[20] J. Rouquerol, D. Anvir, C.W. Fairbridge, et al., Recommendations for the characterization of porous solids, Pure and Applied Chemistry 66 (8) (1994) 1739–1758.
[21] D.S. Ensor, M.E. Mullins, The fractal nature of dendrites formed by the collection of particles on fibers, Particle Characterisation 2 (1985) 77–78.
[22] E. Schmidt, Elektrische Beeinflussung der Partikelabscheidung in Oberflächenfiltern, Ph.D. thesis, Faculty of Chemical Engineering, Karlsruhe University of Technology, Karlsruhe, Germany (1991).
[23] M. Ferer, D.H. Smith, Modeling of backpulse filter cleaning: the small particle filter cake fragments, Aerosol Science and Technology 29 (3) (1998) 246–256.